DOI: 10.13009/EUCASS2023-022
Aerospace Europe Conference 2023 – 10TH EUCASS – 9TH CEAS

ReFEx: Reusability Flight Experiment - Architecture and Algorithmic Design of the GNC Subsystem

Jose Luis Redondo Gutierrez⋆†, *Pablo Bernal Polo*⋆, *Björn Gäßler*⋆⋆, *Johannes Robens*⋆⋆,
Paul Acquatella⋆⋆, *David Seelbinder*⋆, *Stephan Theil*⋆
⋆ *DLR, Institute of Space Systems, Bremen, Germany*
⋆⋆ *DLR, Institute of System Dynamics and Control, Oberpfaffenhofen, Germany*
Address
jose.redondogutierrez@dlr.de · pablo.bernalpolo@dlr.de · bjoern.gaessler@dlr.de
johannes.robens@dlr.de · paul.acquatella@dlr.de · david.seelbinder@dlr.de · stephan.theil@dlr.de
†Corresponding author

Abstract

The German Aerospace Center (DLR) "Reusability Flight Experiment" (ReFEx) aims to demonstrate the Guidance, Navigation, and Control (GNC) capabilities for an aerodynamically controlled Reusable Launch Vehicle (RLV) stage. The GNC subsystem is responsible for maintaining stability and steering the vehicle to achieve a target state, specifically transitioning from the supersonic to subsonic flight regime. This objective is accomplished through: 1) planning and updating a feasible trajectory from separation up to the target state (Guidance); 2) estimation of the vehicle's current state by leveraging sensor measurements (Navigation); and 3) tracking the guidance's attitude commands while maintaining vehicle's stability using the actuators (Control). This paper provides a comprehensive overview of the algorithms employed within these modules, their integration into the GNC architecture, and an evaluation of their performance. The results demonstrate that the GNC algorithms meet the requirements, while acknowledging the need for further improvements in the accuracy of the navigation solution. By showcasing the GNC capabilities of the ReFEx project, this research contributes to advancing the field of aerodynamic control for RLV stages.

1. Introduction

The complexity and cost of launch vehicles makes them a major target when aiming at reducing the expensiveness of access to space. Reusing these vehicles, either partly or completely, is among the strategies that are currently studied and implemented to reduce the share of the launch in the total cost of the mission. The German Aerospace Center (DLR) is currently conducting several missions involving reusable launch vehicles, including both VTVL (Vertical Take-off Vertical Landing), such as CALLISTO [4] [15], and VTHL (Vertical Take-off Horizontal Landing), such as ReFEx (Reusability Flight Experiment). This paper focuses on the latter.

ReFEx is part of the DLR effort to develop future winged reusable launcher stages and vehicles with reentry capabilities. The mission focuses on the reentry phase of a Vertical Takeoff and Horizontal Landing (VTHL) vehicle. The vehicle relies on its aerodynamic properties to reduce the kinetic energy during the reentry phase. One of the main objectives of the mission is to demonstrate autonomous GNC capabilities for aerodynamically controlled reentry vehicles. The demonstration flight is planned for 2024 from the Koonibba Test Range in Australia.

This paper gives an overview on the different GNC algorithms implemented for this mission as well as on the simulation environment used to develop and verify them. The paper begins by giving an introduction to ReFEx, describing the vehicle and the different phases of the mission. Section 3 provides an overview of the functional structure of the GNC system, showing the main modules, their functionalities and the interfaces between them. Sections 4, 5 and 6 dive into the Guidance, Navigation and Control strategies respectively. They provide an insight on the main design drivers and challenges, as well as the solutions implemented for this mission. The simulation environment used to verify the performance of the algorithms is introduced in Section 7.

DOI: 10.13009/EUCASS2023-022

2. Mission

ReFEx is a demonstrator mission that succeeds the DLR SHEFEX II (Sharp Edge Flight Experiment), which was launched in 2012 [5]. ReFEx aims to perform an autonomously controlled and guided flight, following a trajectory representative of a winged RLV (Reusable Launch Vehicle) first stage. The vehicle will transition from hypersonic speeds (above Mach 5) down to the subsonic regime (below Mach 0.8). This section introduces the vehicle and the trajectory for the mission. A more comprehensive overview of the mission can be found in [13] [1].

2.1 Trajectory

Figure 1 illustrates the sequence of events for the mission, along with some preliminary details. The figure highlights several phases: 1) the launch phase, 2) the experimental phase until Entry Interface (EI), 3) the experimental phase between EI and End of Experiment (EoE), and 4) the experimental phase after EoE.

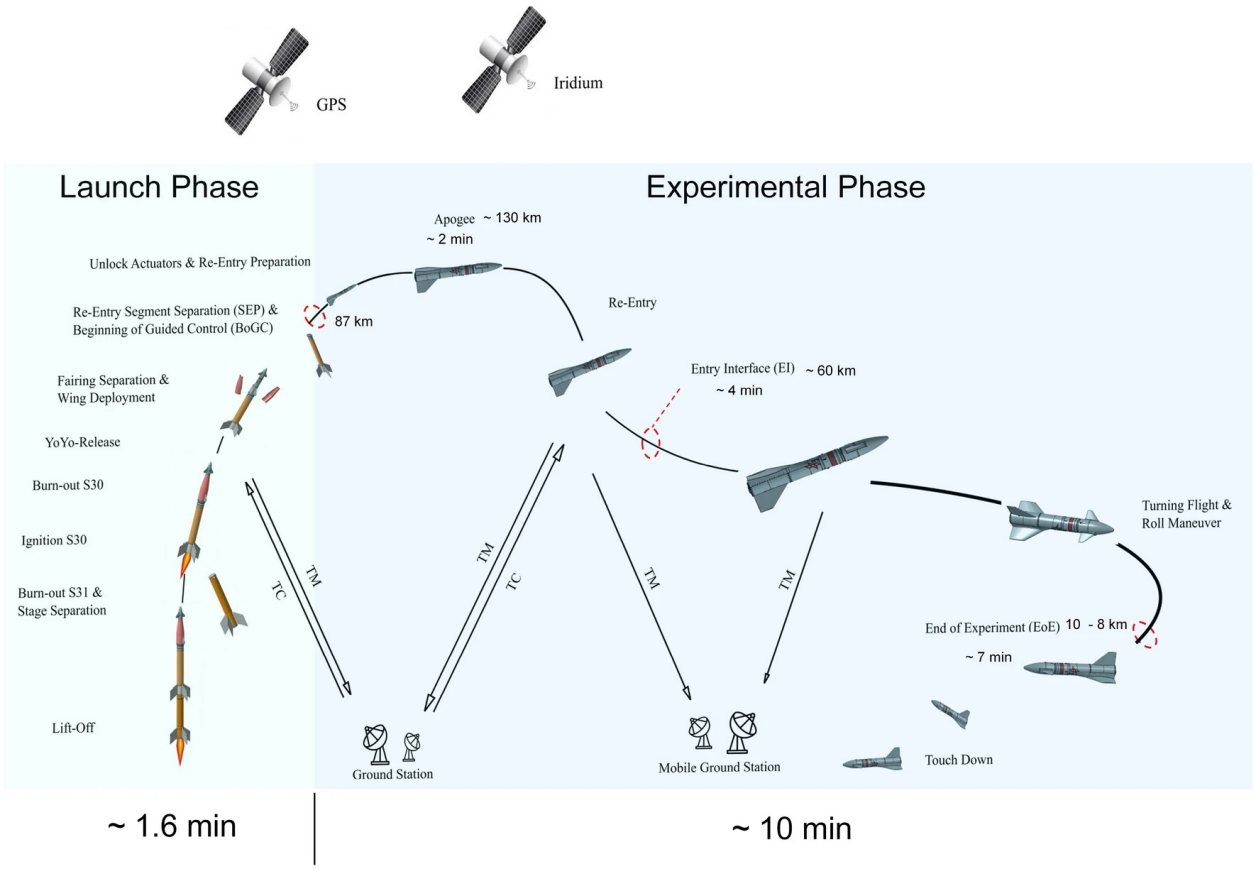

Figure 1: Mission architecture & flight events [1].

A Brazilian solid propellant two-stage rocket (VSB-30) will be used during the launch phase; this rocket is unguided and only passively stabilized by a fast longitudinal-axis angular (roll) rate. This fast rotation requires special consideration from the Navigation system perspective regarding the type of sensors to use, since it can negatively affect the accuracy of the solution at separation. Furthermore, as the rocket is unguided, the position and velocity at separation can differ considerably from the nominal values, posing a challenge to the Guidance system. During the launch phase, most of the Re-Entry segment is covered using a fairing to minimize its aerodynamic effect. Only the Navigation subsystem is active during this phase, while the Guidance and Control remains inactive until the Re-entry segment separation. After the two stages are burned out, the rocket is spun down using a Yo-Yo system, and the fairing and rocket are jettisoned.

After separation until the Entry Interface (EI) is reached, the atmosphere is not dense enough to aerodynamically control the motion of the vehicle; this leads to a ballistic trajectory during the exoatmospheric flight phase. Due to the absence of non-inertial forces, the measurements of the IMU accelerometers can't be coupled with the attitude estimation within the Navigation filter. Therefore, the most relevant improvements in the attitude estimation in this phase come from the

DOI: 10.13009/EUCASS2023-022

sun sensors. During this ballistic (exoatmospheric) flight phase, the vehicle's position and velocity diverge further from their nominal values. Also, as the aerodynamic actuators are uneffective due to the lack of dynamic pressure, the RCS is used to control the attitude of the vehicle by means of cold-gas thrusters. The objectives driving the GNC design for this phase are: 1) to detumble the vehicle after separation, 2) to acquire the sun to improve the attitude information in the navigation solution, and 3) to reach EI with the desired entry attitude.

The EI is defined on a dynamic pressure threshold that guarantees that the vehicle attitude is aerodynamically controllable. The coupling of translational and rotational motion within the navigation filter results in a significant improvement in the navigation solution. During this phase, the objective is to utilize the aerodynamic forces to correct the trajectory, compensating for the dispersion of the vehicle's position and velocity at separation, as well as other uncertainties and errors. The desire EoE conditions on Mach number and kinetic energy can be mapped to coupled ellipsoids in position and velocity. Following EoE, the guidance aims to dissipate as much energy as possible to minimize ground impact while avoiding no-landing zones, such as lakes, sandpits, or populated areas.

2.2 Vehicle

The Re-Entry segment of ReFEx has approx. 400 kg of mass and a longitudinal length of 2.7 m. The wingspan is 1.1 m and the diagonal terms of the moment of inertia are approx. 15 kgm^2 for the longitudinal axis and 240 kgm^2 for the other two axes. A section view of the vehicle is shown in Figure 2.

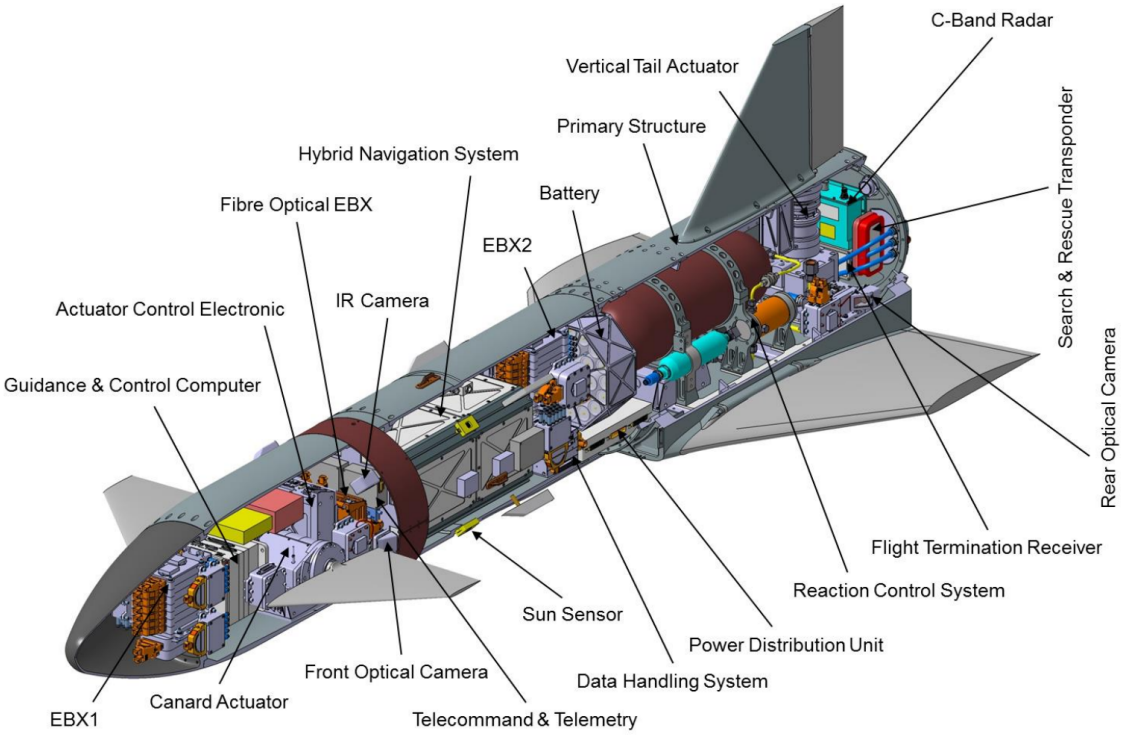

Figure 2: Section view of the Re-Entry segment of ReFEx [1].

Several iterations of the vehicle's shape have been undertaken throughout the history of the mission to meet the aerodynamic requirements for the intended range of velocities, ranging from hypersonic to subsonic. The current design comprises two fixed wings positioned at the rear of the vehicle, a fin with an attached vertical tail actuator (rudder), and two canards located near the nose of the vehicle to allow 3-axis attitude controls during the atmospheric flight phase.

Since translational motion is primarily controlled by aerodynamic forces, the actuators are solely utilized for managing the vehicle's attitude. Two sets of actuators are employed: 1) RCS (Reaction Control System), consisting of 8 thrusters located at the rear of the vehicle, and 2) aerodynamic actuators, encompassing the aforementioned canards and rudder.

DOI: 10.13009/EUCASS2023-022

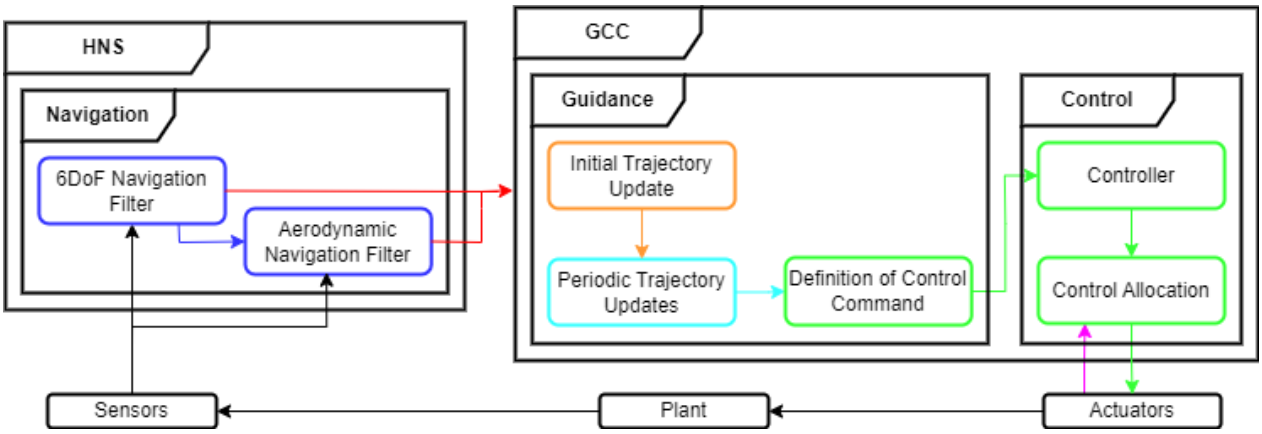

Figure 3: Simplified functional architecture of GNC algorithms for RFX. Different frequencies are represented with different colors: 400 Hz (blue), 80 Hz (red), asynchronous (orange), 0.5 Hz (turquoise), 40 Hz (green), 200 Hz (pink), not applicable/ several frequencies (black).

3. GNC Architecture

This section provides an overview of the different building blocks within the GNC subsystem, as well as how they are organized with respect to each other and what are the main interfaces (see Figure 3). ReFEx's GNC system is divided in two physical On-Board Computers (OBCs): the HNS (Hybrid Navigation System) and the GCC (Guidance and Control Computer). The main interfaces are described in Table 1.

Table 1: Interface summary

Interface	Interface content
Sensors → HNS	Measurements and status from: IMU (Inertial Measurement Unit), sun sensors, GNSS (Global Navigation Satellite System) and FADS (Flush Air Data Sensing system).
HNS → GCC	Estimated values for: position (r), velocity (v), acceleration (a), attitude quaternion (q), angular rate (ω), angular acceleration ($\dot{\omega}$), Mach number (Ma), angle of attack (α), angle of sideslip (β), time derivatives of the angle of attack ($\dot{\alpha}$ and $\ddot{\alpha}$), the angle of sideslip ($\dot{\beta}$ and $\ddot{\beta}$), and the bank angle ($\dot{\mu}$ and $\ddot{\mu}$), dynamic pressure (p), and altitude (h).
Guidance → Control	Reference commands for: α, $\dot{\alpha}$, $\ddot{\alpha}$, β, $\dot{\beta}$, $\ddot{\beta}$, μ, $\dot{\mu}$ and $\ddot{\mu}$.
GCC → Actuators	Control commands for: pressure level of RCS, open/close of each RCS thruster, deflections of right canard (η_r), left canard (η_l) and rudder (ζ).
Actuators → GCC	Measurements of: thrust level of RCS tank, η_r, η_l and ζ.

The HNS runs the navigation algorithms and interfaces with the sensors and with the GCC. The input from the sensors is fused to generate the navigation solution. The fusion takes place via two consecutive Extended Kalman Filters (EKF): 1) the 6DoF filter, that estimates the position, velocity and attitude, and 2) the aerodynamic filter, that estimates aerodynamic quantities such as angle of attack, angle of sideslip and Mach. These filters are executed at 400 Hz and the navigation message is sent at 80 Hz.

The GCC runs the guidance and control algorithms. The guidance algorithms receive the navigation message and perform three main tasks: 1) an initial update of the trajectory after separation to compensate for the deviation w.r.t. the nominal trajectory during the launch phase, 2) periodic updates of the trajectory throughout the reentry phase, to compensate for control and navigation errors as well as modelling uncertainties, and 3) generating the reference signals for the attitude control loop. The periodic updates are performed every 2 seconds and the reference signal is sent to the controller at 40 Hz.

The control algorithms receive the reference command from guidance, the navigation message and the measurements of the internal sensors of the actuators. The torque needed to follow the commanded attitude is computed. The controller output (i.e. commanded torque) is then allocated to either thrusters (exo-atmospheric phase) or aerodynamic deflectors

DOI: 10.13009/EUCASS2023-022

(endo-atmospheric). Both steps are executed at 40 Hz.

4. Guidance Algorithms

The guidance algorithms compute the reference commands for the attitude control loop. The control command schedule has to satisfy constraints given by the vehicle dynamics and the translational and rotational equations of motions.

4.1 Guidance Challenges

There are three main challenges to achieving this objective. Due to the unguided launcher, by the time ReFEx separates from the launcher the trajectory is expected to have diverged considerably from the nominal case. Figure 4a shows the dispersion at separation (in blue) in latitude (ϕ), longitude (λ) and altitude for a Monte Carlo campaign. During the exoatmospheric phase the vehicle has no means to influence its motion and since the trajectory is purely ballistic, the divergence from the nominal trajectory increases further. Figure 4a also shows (in red) the state when a dynamic pressure of 1000 Pa is reached. No meaningful correction of the trajectory via aerodynamic forces can be conducted at lower dynamic pressures. To gain perspective of the distance and size relations, the target ellipsoid is also shown in green, with concentric circles of radius 5, 10 and 15 km.

Secondly, the effect of modeling uncertainties and control and navigation errors accumulates, increasing the divergence w.r.t. the planned trajectory. Figure 4b) shows the errors in position at EoE if the control feedback system tracks a trajectory that is recomputed once to eliminate the state error that has accumulated up to the apogee. Due to the lack of additional corrections to the trajectory, the effect of modelling errors and unknown perturbations is not adequately compensated leading to a considerable deviation from the desired target conditions.

An additional challenge are the aerodynamic limitations of the vehicle. There are combinations of Mach and α where the vehicle is underactuated. Figure 5 shows a trimability analysis in the Mach-α domain for different values of β. The figure shows the areas that are trimmable for different values of β, from 0 (light blue) to 2 degrees (yellow). This analysis is equivalent to that detailed in [12], where the causes and consequences of this phenomenon are discussed. In order to avoid the potentially unstable regions, a flying corridor is defined. The flight corridor, shown in Figure 5 in blue, is flown from high Mach numbers at the beginning of the reentry phase to low Mach numbers at EoE. It minimizes the time spent in the Mach-α regions where the vehicle is underactuated are crossed.

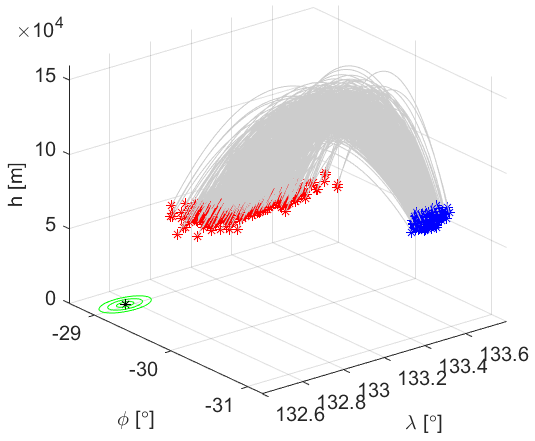

(a) Effect of error at separation [11]. Separation state (blue), EI state (red), EoE target (green).

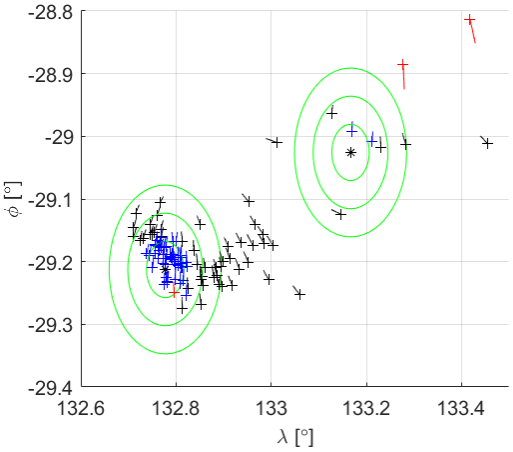

(b) Effect of modeling uncertainties and control and navigation errors in the precision reaching the EoE target. Successful (blue), failed (black) and unstable (red). The EoE targets are shown in greed.

Figure 4: Challenges in relation to guidance algorithms

4.2 Guidance Functionalities

Driven by these challenges, the guidance module implements three functionalities (see figure 3): 1) One major update of the trajectory after separation, 2) periodic minor updates of the trajectory, and 3) generation of a feasible control

DOI: 10.13009/EUCASS2023-022

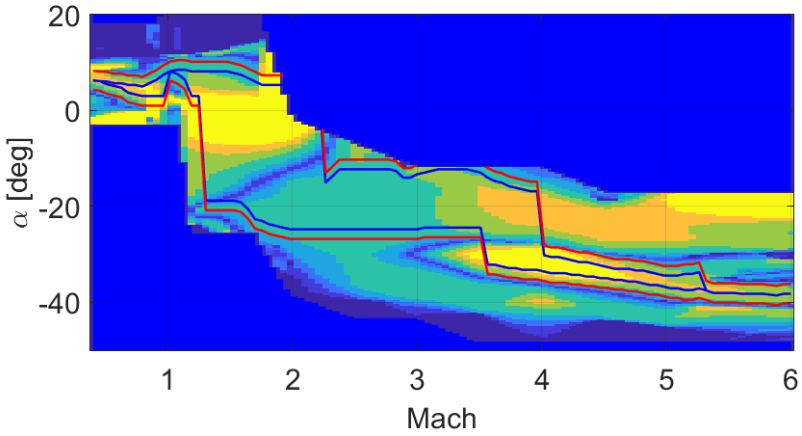

Figure 5: Trimmable regions for β between 0 (dark blue) and 2 (yellow) degrees. Flight corridor for α w.r.t. Mach with (blue) and without (red) safety margin.

command.

The initial trajectory update aims at correcting for the dispersion in position and velocity after separation from the launcher, by generating an updated trajectory leading from the estimated state to the target. This algorithm is explained in [11], and consists of a simplification of the optimal control problem, reducing the profiles of the control variables to a set of control parameters. Defining this set of parameters is not trivial as it limits the solution space. This problem reduction is combined with a function that propagates the trajectory from the initial state while enforcing all existing constraints. This approach is able to transform the problem into an unconstrained optimization problem, which is able to find solutions of similar quality as the full optimal control approach. This problem can then be reduce to and solved by a zero-crossing search. While analyzing the feasibility of trajectories it became apparent that the uncertainty of the state at separation is so large that not for all perturbed conditions a feasible trajectory exists to the desired terminal condition. Therefore, a strategy to define the convergence envelope to the nominal target was integrated in the algorithm. For initial conditions which have no feasible trajectory to the target, or which are marginally feasible through operating the vehicle at the boundary of its controllability space, a secondary fallback target is defined.

The periodic trajectory updates aim at correcting for the accumulating effect of modeling uncertainties and control errors. Similarly as for the full trajectory update, the control variables are expressed as a function of a set of parameters. These parameters, whose definitions are critical as they define the solution space, define both the short term behaviour and the overall profile of the control variables. The problem is then again combined with a propagation function and converted into a non-linear unconstrained optimization problem. Due to the need to periodically update the trajectory, there is not enough time to completely solve the problem and a trade-off between the maximum number of iterations allowed and the frequency of the trajectory updates was conducted. Additional corrections of the control variable profiles after the EoE are made in order to avoid no-landing zones, particularly lakes, and to minimize the vertical impact velocity, via a flare maneuver.

Multiple filters were studied to shape the control command, leading to the decision of using a third-degree low-pass (PT3) filter that ensures that the angles, angular rates and angular accelerations are smooth, while allowing discontinuities in the jerk.

4.3 Guidance Performance

In order to verify the performance of the guidance algorithms two main analyses were performed: 1) accuracy of initial trajectory update, and 2) close-loop performance including periodic trajectory updates. For reference, the requirements for the close-loop performance w.r.t. errors at the end of experiment are, for 3σ: 20 km radius in horizontal position, 1 km in altitude, 100 m/s in velocity and 20° in heading.

The first analysis evaluates the capability of the algorithms to define a trajectory from the state at EI to the one of the targets. Figure 6 contains the results of a Monte Carlo campaign of 1000 runs. The results show that this algorithm is able to find trajectories well within requirements for all cases. Further results are shown in [11].

The seconds analysis contains the closed-loop performance of the GNC algorithms, including all error and uncertain-

DOI: 10.13009/EUCASS2023-022

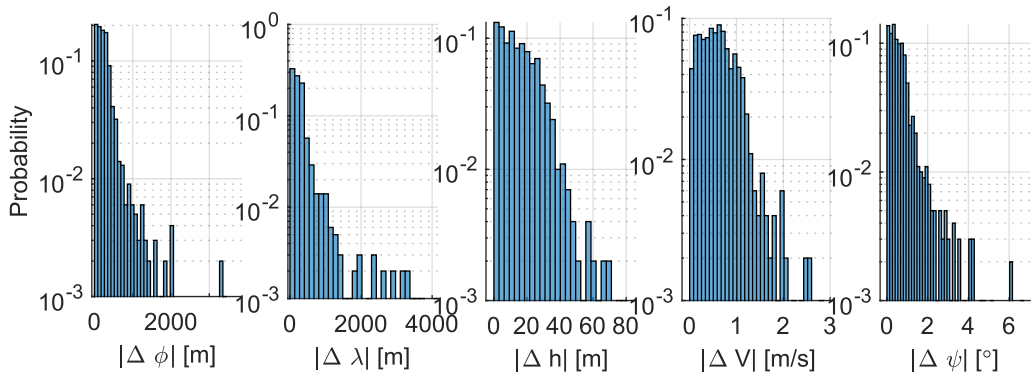

Figure 6: Results of initial trajectory update.

ties. The simulation environment that is the basis for the analysis is detailed in Section 7. The results consists of a Monte Carlo campaign of 200 runs. Out of this 200 runs, there are 5 cases in which the vehicle becomes unstable. These cases are a direct consequence of a lack in navigation accuracy (discussed in Section 5) and are expected to be resolved with the next tuning iteration of the navigation algorithms. Figure 7 shows the error at EoE for the remaining 195 cases. The requirements, shown at the beginning of this subsection, are fulfilled.

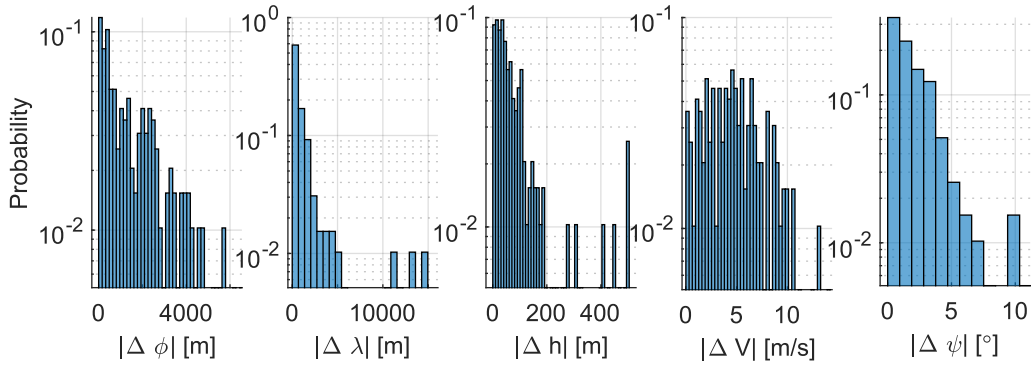

Figure 7: Results of periodic trajectory updates.

5. Navigation Algorithms

The navigation algorithms designed for the ReFEx mission have the main purpose of estimating the state of the ReFEx vehicle. This goal is achieved by exploiting the information contained in the measurements provided by the set of sensors mounted on board:

- The **IMU** provides angular velocity and acceleration measurements. Unlike the traditional design, the IMU that will be used for ReFEx will have four measurement axes (four COTS (Comercial Off-The Shelf) accelerometers and four modified COTS gyroscopes) arranged in a tetrahedral configuration. The measured values are the projections on each axis of the true angular velocity and acceleration, which must be reconstructed from such measured values. The unit will be assembled, integrated, calibrated, and characterized in house.
- The **GNSS** provides position and velocity measurements as three-dimensional vectors. It is based on the flight-proven Phoenix-HD GPS receiver developed at German Space Operations Center (GSOC) specifically for use in space and high-dynamics projects [8, 9]. For the reception of the GPS signals, a GNSS wrap-around antenna with an almost omnidirectional receiving pattern and spin insensitivity is used.
- **Sun sensors** provide the direction of the Sun encoded as two angles. Being based on Micro-Electro-Mechanical Systems (MEMS) fabrication processes, and due to the geometrical dimensions of their design, they have high sensitivity and are highly accurate. There are four of them distributed uniformly around the longitudinal axis of the vehicle to maximize the probability of capturing the sunlight. The units will be calibrated by the manufacturer, characterized in house and re-calibrated if necessary.

DOI: 10.13009/EUCASS2023-022

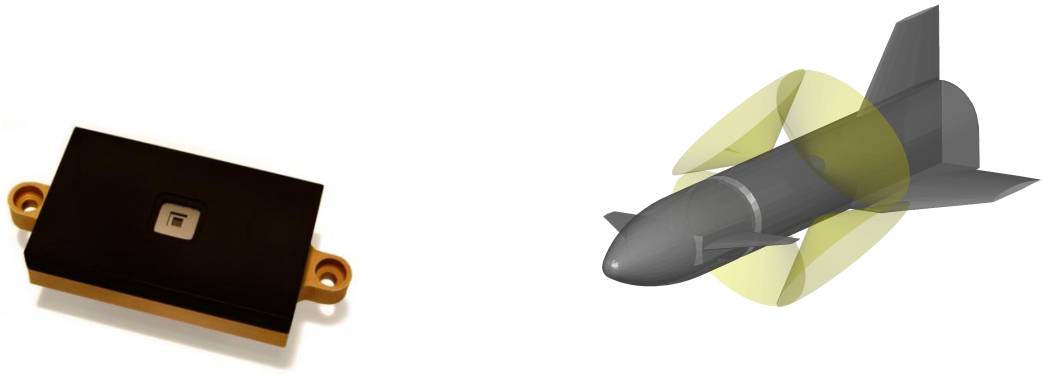

(a) Geometry of a Sun sensor.

(b) Disposition of Sun sensors around ReFEx vehicle.

Figure 8: Sun sensors in ReFEx vehicle.

- The **FADS** provides an array of pressure measurements collected at different positions on the surface of the nose of the vehicle. These pressure measurements are related to aerodynamic variables such as Angle of Attack, Mach number or dynamic pressure, which can be recovered using different methods [17, 2]. The system is being developed by the Institute of Aerodynamics and Flow Technology [6].

State of the art navigation algorithms have been designed and developed to produce an estimation of the state of the ReFEx vehicle. The variables used to build such state can be classified into kinematic variables and aerodynamic variables. The kinematic variables describe the state of the vehicle with respect to Earth. In particular, the kinematic part of the state is composed of attitude, position, velocity, angular velocity and acceleration. On the other hand, the aerodynamic variables describe the state of the vehicle with respect to the Earth's atmosphere. The aerodynamic part of the state is comprised of the attitude of the vehicle with respect to the air path, which decomposes into α and β, and also includes Mach number and dynamic pressure. The combination of all these variables conform the navigation solution.

In order to produce the navigation solution, the information contained in sensor measurements needs to be processed, merged and transfigured into the aforementioned variables. We adopt the Kalman filter framework as the main tool used for estimation. A Kalman filtering library concept is being developed and tested in the ReFEx simulator. The Kalman filtering library is designed following the Object Oriented Programming paradigm (OOP), and exploits software design patterns, optimization patterns, and extensive testing. It aims to establish a simple and modular framework in which to integrate the experience acquired in multiple projects, and thus facilitate the development of the navigation algorithms described in this section, and those of future projects. For ReFEx, the navigation algorithms are essentially composed of two Extended Kalman filters: the first one estimates the kinematic state, and a second one uses the output from the first to estimate the aerodynamic variables. Quaternions are the optimal choice to represent the rotation transformation that describes the orientation of a vehicle [3], but this is especially true for the ReFEx mission due to its high dynamics and range of possible attitudes.

In particular, the estimation of the attitude is both challenging and critical, as the aerodynamic forces are dependent on the attitude. The period prior to EI is specially challenging. At this point, the vehicle becomes aerodynamically controllable and it is essential to ensure an accurate attitude estimation before transitioning to aerodynamic control of the vehicle. Achieving the desired accuracy is difficult due to a number of reasons. The gyroscope scale factor errors together with the high rotational rates reached during ascent produce considerable error in angular velocity measurements. This leads to a substantial accumulated attitude error at the end of the ascent.

Once out of the influence of the atmosphere, the Sun direction is the only source of attitude information. However, a direction provides only partial information about the absolute orientation. This means that regardless of how long the Sun is acquired, the full absolute orientation will not be observable. When the aerodynamic forces begin to be significant, the accelerations measured by the IMU result in an integrated position that is coupled with the GPS measurements. This makes the orientation observable again. However, for some trajectories this happens too late, giving G&C no time to react. In these cases, the dynamic pressure starts generating aerodynamic forces while the navigation error in attitude is still considerably above 20°. This leads to large errors in the aerodynamic angles and, consequently, the aerodynamic forces and torques. This currently leads to a probability of failure of roughly 5%, which is expected

DOI: 10.13009/EUCASS2023-022

to be solved in future iterations of the navigation algorithms. Several options are being investigated, including: 1) extension of the filter state to include errors sources of the IMU (e.g. misalignment and bias), and 2) modification of launch date and time to minimize the accumulative angular error in the non-observable axis during the ascent phase.

During the atmospheric flight the effect of errors in the attitude is considerably stronger, as it is directly reflected in the aerodynamic forces and torques. Furthermore, as some navigation variables are expresses w.r.t. the local air frame (i.e. angle of attack and angle of sideslip), there is a non-negligible effect of the wind. The measurements from FADS are used to estimate the velocity of the wind, compensating for its effect. Due to the position of FADS (in the nose of the vehicle) and the thermal bending of the vehicle during the flight, there are additional error (besides the accuracy of the pressure sensors).

Figure 9 shows the navigation error from launch until 100 s after EI. The colorful dots represent instants in which a sun sensor measurement is processed. Each color represents one of the different Sun sensors mounted in the ReFEx vehicle (see Figure 8b. During the ascent, up to $t = 100$ s, both the covariance and error increase considerably. After separation the total error remains approximately the same until the sun is acquired at t$\approx$ 120 s. this initial sun acquisition reduces the error considerably. From this point until t$\approx$ 300 s the error in each axis varies but the total attitude error remains the same, and further sun acquisitions have no meaningful effect. When the aerodynamic forces become significant (around $t = 300$ s) the navigation filter converges to a more accurate solution.

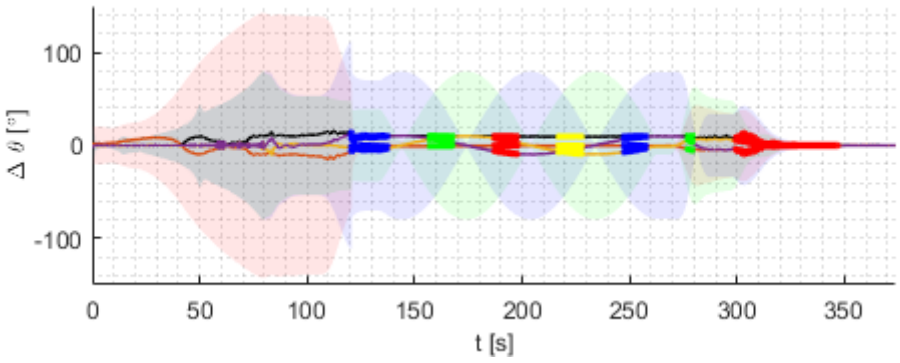

Figure 9: Navigation errors during exoatmospheric phase. Colored lines are the components of the rotation vector that represents attitude error. Black line is the norm of the rotation vector that represents attitude error. The background color represents the covariance evolution.

Figure 10 shows the evolution of the observable angular error, w.r.t. the sun. It can be observed that the sun sensor measurements reduce the observable error as soon as a valid measurement is produced. The non-observable error (i.e. rotation around the Sun direction axis) remains high until entering the atmosphere.

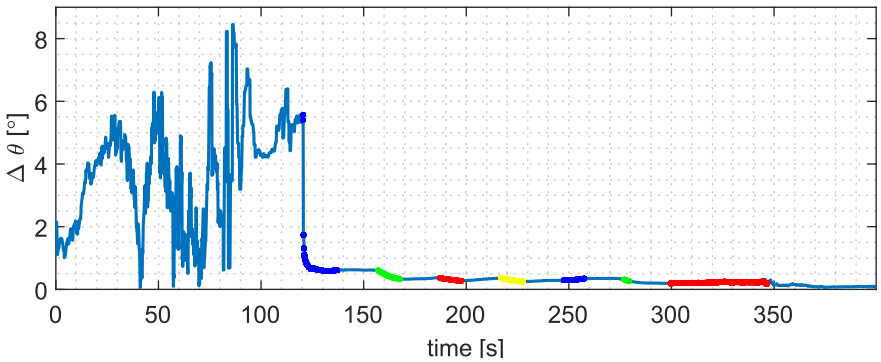

Figure 10: Time evolution of observable (by sun sensors) attitude error.

Figure 11 shows the evolution of the error in angle of attack for a Monte Carlo campaign of 200 runs (the same shown in figure 7). The information is presented in two subfigures in order to facilitate the visualization of the results. As explained in Figure 9, the error is reduced once non-gravitational forces (i.e. aerodynamic forces) are present. For ReFEx, this occurs between 300 and 330 s after launch, depending of the ascent trajectory. Once the navigation solution

DOI: 10.13009/EUCASS2023-022

has converged, the error is bounded between $-1.5°$ and $1.5°$. The angular bias is caused by the thermal bending, which is not modelled in the filter.

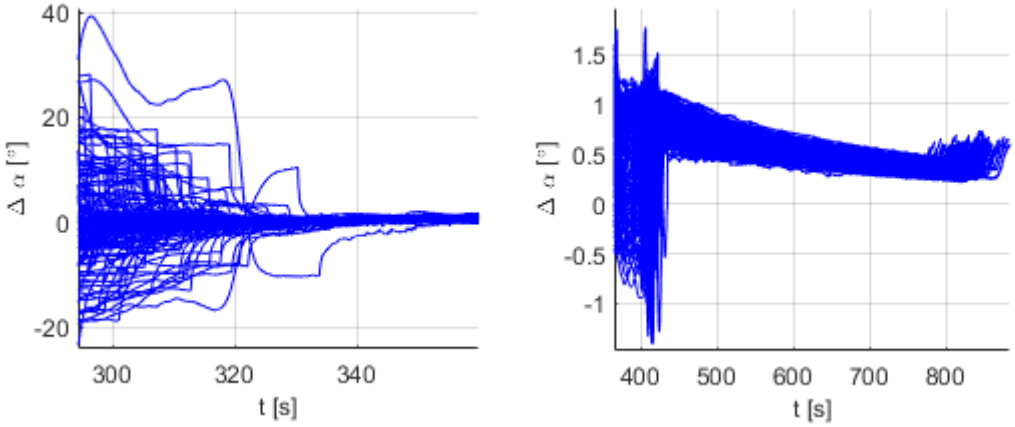

(a) (b)

Figure 11: Error in α: (a) convergence after EI, and (b) endo-atmospheric flight.

6. Control Algorithms

The ReFEx controller is divided into two control subsystems, one for the exoatmospheric flight phase and one for aerodynamically controlled atmospheric flight. During the exoatmospheric flight phase the dynamic pressure is too low to produce considerable aerodynamic forces and moments for vehicle control. Therefore the vehicle's attitude is manipulated using the cold gas thrusters of a RCS. As the atmosphere becomes dense enough to generate considerable aerodynamic forces and moments the vehicle enters the atmospheric flight phase. Transition between the two control systems takes place when the aerodynamic pressure reaches a threshold that enables control authority using the aerodynamic control surfaces.

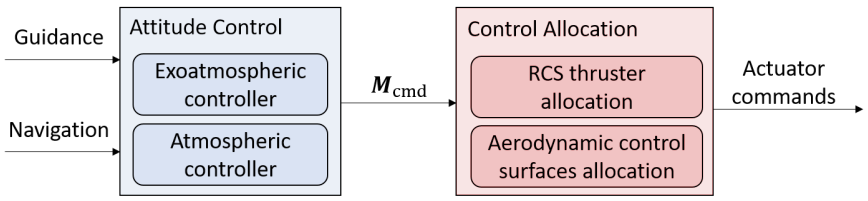

Figure 12: Basic controller structure

Figure 12 shows the ReFEx basic controller structure. An attitude controller calculates a commanded moment based on navigation information and the guidance reference signal. This commanded moment is mapped to RCS thruster on/off commands or aerodynamic control surfaces deflections by a control allocation.

6.1 Exoatmospheric Control System

During the exoatmospheric flight phase the guidance system provides fixed reference states. To enable a smooth transition between the vehicle's current and the desired reference state a trajectory is planned by means of spherical linear interpolation and polynomial progression. The resulting trajectory uses the shortest rotational direction and ensures that the commanded torques do not exceed the thrusters' capabilities. Due to the limited amount of fuel and the discrete behavior of cold gas thrusters, a PD-controller including a deadband is implemented. The controller is extended by a feedback linearization term such that controller gains can be approximately determined by pole placement. As a result, it can be guaranteed that the vehicle transitions without overshoots.

In order to allocate commanded torques to discrete thruster on/off-commands, a pulse modulation scheme is applied for each body axis. Based on the work of Kienitz et al [7], the pulse-width pulse-frequency (PWPF) modulation explicitly consider switching restrictions like minimum pulse duration and minimum rest between successive pulses.

DOI: 10.13009/EUCASS2023-022

It additionally corrects for time-delayed actuator action caused by the time it takes until a stationary flow through a thruster is established. In contrast to classical PWPF modulators the implemented pulse modulator is capable to accurately realize the commanded torques without approximation losses. Individual thruster commands are allocated by a switching logic which aims to use the maximum number of thrusters that can produce the desired torques. This results in fast, yet accurate maneuvers and a fault tolerance for the failure of up to two thrusters in the roll and pitch channel. A detailed description of the exoatmospheric control system including an evaluation of its performance is published in [14].

The performance of the exoatmospheric control system is demonstrated in Figure 13, which depicts the total angle error θ_t and the norm of the measured angular velocity ω_m for a nominal simulation without perturbations or disturbances. The total angle error is defined as the Euler angle of a single axis rotation that is needed to rotate from the current to the final (reference) attitude. Within Figure 13 the individual modes of the exoatmospheric flight phase can be detected. First, residual angular rates remaining after de-spin and separation are successfully damped. Thereafter, the vehicle reorients and reaches the desired attitude at roughly t=150 s, indicated by the decreasing error in total angle. To calibrate the navigation system, the vehicle rotates with a constant rate before returning to a stationary state. These maneuvers can be recognized in Figure 13b between t=150 s and t=275 s. Finally, the vehicle reorients to take the correct attitude for reentry as can be seen by the second peak in total angle error and follows continuous guidance commands until aerodynamic actuators can be used to control the vehicle.

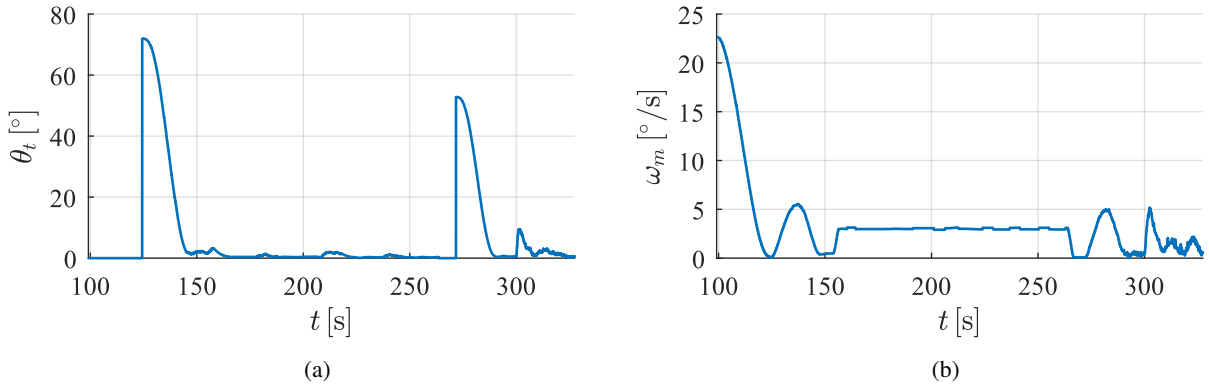

Figure 13: Functionality of exoatmospheric control system by selected states. (a) Total angle error and (b) measured angular rate

6.2 Atmospheric Control System

During the atmospheric flight phase the control system aims to robustly track the constantly updated attitude reference trajectory provided by the guidance system. This is especially challenging since the flight conditions range over a high mach and angle of attack envelope with actuator control effectiveness significantly changing including areas of control reversals and singularities in the control effectiveness.

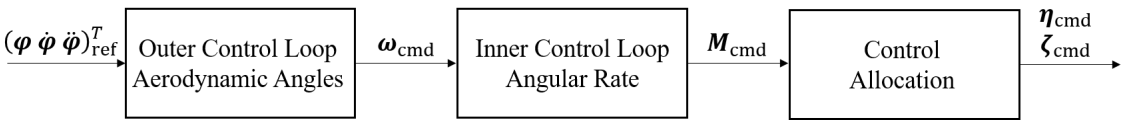

Figure 14: Cascaded controller structure for the aerodynamic flight phase

To cope with these challenges, a model- and sensor-based cascaded control system based on incremental nonlinear dynamic inversion (INDI) control strategy is applied [16]. The control system as shown in Figure 14 consists of a two-loop cascaded controller where the outer loop receives reference aerodynamic angles $\boldsymbol{\varphi} = (\mu\ \alpha\ \beta)^T_{\text{ref}}$ and their derivatives as input from Guidance. A linear controller combining feed-forward (FF) and feedback (FB) elements provides the pseudo-control reference signals to the nonlinear dynamic inversion which calculates a commanded angular rate $\boldsymbol{\omega}_{\text{cmd}}$ (outer loop). The output angular rate serves as input to the inner control loop which applies the same structure as the outer loop combining a linear controller with FF and FB elements and an incremental nonlinear dynamic inversion to calculate commanded moments $\boldsymbol{M}_{\text{cmd}}$. This controller structure enables fast signal tracking as well as compensation

DOI: 10.13009/EUCASS2023-022

of uncertainties and disturbance rejection while rendering gain scheduling unnecessary. A control allocation based on INDI with estimated angular accelerations and local control effectiveness matrices, maps the commanded moments to aerodynamic control surface deflections. To avoid actuator saturation and unintended behavior in the vicinity of control reversals the control allocation is combined with a singularity avoidance mechanism using a constrained damped least squares methodology. An initial version of the aerodynamic control allocation can be found in [12]. Further publications are expected in this topic.

The performance of the atmospheric control system is shown in Figure 15 for the nominal case. Only bank angle μ and angle of attack α are presented, since the angle of sideslip is always commanded to be zero and is stabilized by the control system with an average error of 0.06° deg and a maximum error of 0.5°. In general, the commanded bank angle and angle of attack are tracked accurately over the whole atmospheric flight with an average error of 0.02 and 0.08°, respectively. Additionally, expected critical phases of the flight are stabilized by the control system. The angle of attack reaches its maximum error of degrees during the highest dynamic pressure at roughly t≈ 350 s, while the bank angle error has its maximum with 0.4° deg during the two singularities in the control effectiveness shortly thereafter. Furthermore, the roll maneuver at around t≈ 450 s, indicated by the large change in bank angle and angle of attack as well as the flare maneuver at the end of the flight are executed successfully.

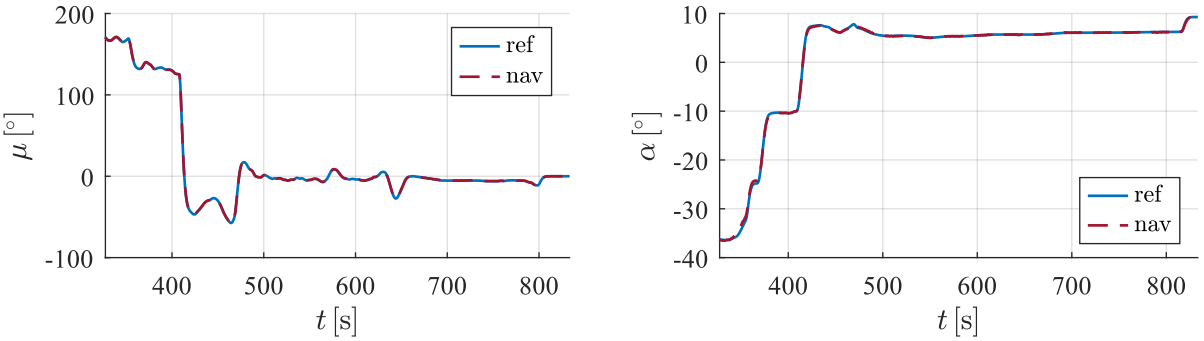

Figure 15: Comparison of commanded and measured aerodynamic states. (a) Bank angle and (b) angle of attack

7. Simulation Environment for MiL

The ReFEx Closed-Loop Simulator provides the means to verify the performance of the GNC as a whole as well as of the different systems that integrate it, i.e. Guidance, Navigation and Control. The top-level structure of the simulator is shown in figure 16. The blue-colored blocks represent the GNC software that is to be verified using this tool. The rest of the blocks contains models of the the different actuators and sensors, the vehicle and the environment.

This simulator provides the capability of running complete Closed-Loop end-to-end simulation from launch to touchdown. This can be used to test the performance of the complete GNC system throughout the mission. In addition, multiple configurations/alternatives can be defined to perform different analyses and evaluate compliance with different requirements.

1. Assume perfect navigation. The navigation solution is equal to the true state. This configuration enables defining and testing requirements related to the performance of the guidance and control algorithms independently from the navigation system.

2. Define the attitude directly as commanded by guidance. Only the translational movement is propagated. The control, control allocation and actuators are bypassed. This setup adds the possibility of investigating the performance of the guidance strategy, without the influence of control errors. This configuration is used for certain parts of the flight safety analysis, presented in [10].

3. Fix the position and velocity and propagate only attitude dynamics. Position and velocity are fixed at a point on the (nominal) trajectory and only the rotational motion of the vehicle is propagated. The guidance command is predefined. With this configuration, the performance of the control algorithms can be studied in particular parts of the trajectory. This ease the tuning of the controller, by isolating the most critical phases of the mission.

DOI: 10.13009/EUCASS2023-022

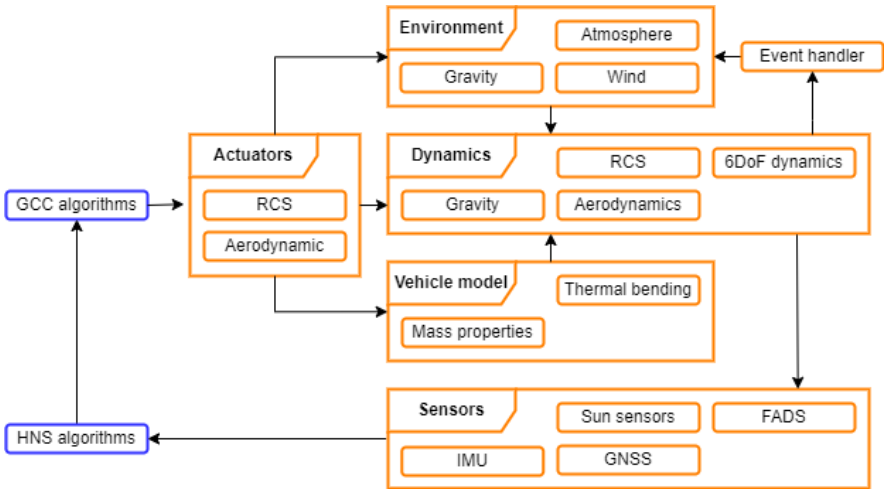

Figure 16: Simplified functional architecture of the Closed-Loop Simulator developed for ReFEx. In blue the GNC algorithms, in orange the modeled plant.

4. Bypass control allocation and actuators. The torque commanded by the control system is directly applied over the vehicle. This allows to investigate separately the performance of the controller and of the control allocation.

The simulator framework allows to perform Monte-Carlo campaigns. Among the parameters that are perturbed for these analyses are: 1) Initial state (position, velocity, attitude and angular rates), 2) Atmosphere (including density, temperature, pressure and wind), 3) Mass properties of the vehicle, 4) Aerodynamic properties of the vehicle, 5) Sensor properties, and 6) Actuators properties.

8. Conclusions

This paper presented an overview of the GNC building blocks for the DLR mission ReFEx. Challenges and solutions associated with the GNC development have been introduced. The selected algorithms and functionalities can be summarized as follows. The guidance algorithms conduct on-board trajectory updates in order to correct deviations with respect to the nominal trajectory. To achieve this, an optimal control problem is reduced to an unconstrained non-linear optimization problem, which is then solved using a root finding search. The navigation algorithms consist of two consecutive Extended Kalman Filters (EKFs), one for the 6DoF dynamics and the other for the aerodynamic variables. The flight control algorithms (attitude control and control allocation) are implemented for the different phases of the mission; these include a PD controller combined with partial dynamic inversion and a pulse-width pulse-frequency (PWPF) modulation for the exoatmospheric phase, and an incremental nonlinear dynamic inversion attitude controller for the atmospheric phase. These algorithms are tested in a reconfigurable 6 dof closed-loop simulator environment.

References

[1] Waldemar Bauer et al. “DLR reusability flight experiment ReFEx”. In: *Acta Astronautica* 168 (2020), pp. 57–68.
[2] Ethan Baumann et al. “X-43A flush airdata sensing system flight-test results”. In: *Journal of Spacecraft and Rockets* 47.1 (2010), pp. 48–61.
[3] Pablo Bernal-Polo and Humberto Martınez-Barberá. “Kalman filtering for attitude estimation with quaternions and concepts from manifold theory”. In: *Sensors* 19.1 (2019), p. 149.
[4] Etienne Dumont et al. “CALLISTO: A Prototype Paving the Way for Reusable Launch Vehicles in Europe and Japan”. In: (2022).
[5] Thino Eggers. “The Shefex II experimental re-entry vehicle: Presentation of flight test results”. In: *28th International Congress of the Aeronautical Science (ICAS)*. 2012.
[6] Andreas K. Flock et al. “Planned Wind Tunnel Experiments at DLR Köln for the Reusability Flight Experiment (ReFEx)”. In: *International Conference on Flight Vehicles, Aerothermodynamics and Re-entry Missions & Engineering*. 2019. URL: https://elib.dlr.de/129445/.
[7] Karl Heinz Kienitz and Johann Bals. “Pulse modulation for attitude control with thrusters subject to switching restrictions”. In: *Aerospace Science and Technology* 9 (2005).

DOI: 10.13009/EUCASS2023-022

[8] Markus Markgraf and Oliver Montenbruck. “Phoenix-HD—a miniature GPS tracking system for scientific and commercial rocket launches”. In: *6th international Symposium on Launcher Technologies*. 2005, p. 5.

[9] Oliver Montenbruck and Eberhard Gill. “Phoenix-XNS-a miniature real-time navigation system for LEO satellites”. In: (2006).

[10] Jose Luis Redondo Gutierrez, Leonid Bussler, and Peter Rickmers. “ReFEx: Reusability Flight Experiment - Flight Safety Analysis”. In: 10th European Conference for Aeronautics and Space Sciences (EUCASS). 2023.

[11] Jose Luis Redondo Gutierrez, David Seelbinder, and Stephan Theil. “Design of ReFEx Guidance: Trajectory Correction after Ascent”. In: *AIAA SCITECH 2023 Forum*. 2023, p. 1995.

[12] Jose Luis Redondo Gutierrez et al. “Design of a Control Allocation Solution for the Winged Reusable Launch Vehicle ReFEx”. In: *AIAA Scitech 2022 Forum*. 2022, p. 1842.

[13] Peter Rickmers et al. “The Reusability Flight Experiment–ReFEx: From Design to Flight–Hardware”. In: *IAC. International Aeronautical Congress 2021*. 2021.

[14] Johannes Robens and Björn Gäßler. “ReFEx: Reusability Flight Experiment - Design of an Exoatmospheric Control System”. In: 10th European Conference for Aeronautics and Space Sciences (EUCASS). 2023.

[15] Marco Sagliano et al. “Unified-Loop Structured H-Infinity Control for Aerodynamic Steering of Reusable Rockets”. In: *Journal of Guidance, Control, and Dynamics* 46.5 (2023), pp. 815–837.

[16] S. Sieberling, Q P Chu, and J A Mulder. “Robust Flight Control Using Incremental Nonlinear Dynamic Inversion and Angular Acceleration Prediction”. In: *Journal of Guidance, Control and Dynamics, Vol. 33, No. 6*. 2010.

[17] Stephen Whitmore, Brent Cobleigh, and Edward Haering Jr. “Design and calibration of the X-33 flush airdata sensing (FADS) system”. In: *36th AIAA aerospace sciences meeting and exhibit*. 1998, p. 201.